ARMY RESEARCH LABORATORY

Combustion Synthesis Reaction Behavior of Cold-Rolled Ni/Al and Ti/Al Multilayers

by Laszlo J. Kecskes, Xiaotun Qiu, Ranran Liu, Jesse H. Graeter, Shengmin Guo, and Jiaping Wang

NOTICES

Disclaimers

The findings in this report are not to be construed as an official Department of the Army position unless so designated by other authorized documents.

Citation of manufacturer's or trade names does not constitute an official endorsement or approval of the use thereof.

Destroy this report when it is no longer needed. Do not return it to the originator.

Army Research Laboratory

Aberdeen Proving Ground, MD 21005-5069

Combustion Synthesis Reaction Behavior of Cold-Rolled Ni/Al and Ti/Al Multilayers

Laszlo J. Kecskes
Weapons and Materials Research Directorate, ARL

Xiaotun Qiu
Arizona State University

Ranran Liu, Jesse H. Graeter, and Shengmin Guo
Louisiana State University

Jiaping Wang
Tsinghua University

REPORT DOCUMENTATION PAGE

Form Approved
OMB No. 0704-0188

Public reporting burden for this collection of information is estimated to average 1 hour per response, including the time for reviewing instructions, searching existing data sources, gathering and maintaining the data needed, and completing and reviewing the collection information. Send comments regarding this burden estimate or any other aspect of this collection of information, including suggestions for reducing the burden, to Department of Defense, Washington Headquarters Services, Directorate for Information Operations and Reports (0704-0188), 1215 Jefferson Davis Highway, Suite 1204, Arlington, VA 22202-4302. Respondents should be aware that notwithstanding any other provision of law, no person shall be subject to any penalty for failing to comply with a collection of information if it does not display a currently valid OMB control number.
PLEASE DO NOT RETURN YOUR FORM TO THE ABOVE ADDRESS.

1. REPORT DATE (DD-MM-YYYY)	2. REPORT TYPE	3. DATES COVERED (From - To)
April 2011	Final	January 2006–January 2008

4. TITLE AND SUBTITLE	5a. CONTRACT NUMBER
Combustion Synthesis Reaction Behavior of Cold-Rolled Ni/Al and Ti/Al Multilayers	
	5b. GRANT NUMBER
	5c. PROGRAM ELEMENT NUMBER

6. AUTHOR(S)	5d. PROJECT NUMBER
Laszlo J. Kecskes, Xiaotun Qiu,* Ranran Liu,† Jesse H. Graeter,† Shengmin Guo,† and Jiaping Wang‡	1L162618AH84
	5e. TASK NUMBER
	5f. WORK UNIT NUMBER

7. PERFORMING ORGANIZATION NAME(S) AND ADDRESS(ES)	8. PERFORMING ORGANIZATION REPORT NUMBER
U.S. Army Research Laboratory ATTN: RDRL-WMM-F Aberdeen Proving Ground, MD 21005-5069	ARL-TR-5507

9. SPONSORING/MONITORING AGENCY NAME(S) AND ADDRESS(ES)	10. SPONSOR/MONITOR'S ACRONYM(S)
	11. SPONSOR/MONITOR'S REPORT NUMBER(S)

12. DISTRIBUTION/AVAILABILITY STATEMENT

Approved for public release; distribution is unlimited.

13. SUPPLEMENTARY NOTES

*Arizona State University, Tempe, AZ, 85287; †Louisiana State University, Baton Rouge, LA, 70803; ‡Tsinghua University, Beijing, People's Republic of China, 100084

14. ABSTRACT

A two- or three-stage combustion synthesis reaction process was observed in cold-rolled Ni/Al and Ti/Al multilayer foils. The phase evolution sequence from the two foil types was studied by differential scanning calorimetry (DSC). Several exothermic peaks were identified from the DSC thermograms. Subsequently, the foils were heated to each peak temperature to identify the reaction product associated with each peak. X-ray diffraction and scanning electron microscopy analyses were used to further discern the thermal events, whether they corresponded to intermediate or final reaction products. The Ni/Al foils went through three reaction stages. In the first stage, Al_3Ni was formed as the reaction product. During the second stage, the part of the foil underwent thermal explosion. In the last stage, the heat released by the thermal explosion triggered a self-propagating high-temperature synthesis reaction that resulted in the formation of AlNi. In contrast, the Ti/Al foils experienced only two reaction stages. In the first, the reaction zone propagated across the foil with formation of Al_3Ti at the Ti/Al interface. Then, a thermal explosion reaction occurred in the part of foil that was heated, resulting in many different phases.

15. SUBJECT TERMS

self-propagating high-temperature synthesis, cold rolling, Ni, Al, nickel aluminides, Ti, titanium aluminides, differential scanning calorimetry (DSC), scanning electron microscopy, reactive multilayered foils

16. SECURITY CLASSIFICATION OF:			17. LIMITATION OF ABSTRACT	18. NUMBER OF PAGES	19a. NAME OF RESPONSIBLE PERSON
					Laszlo J. Kecskes
a. REPORT	b. ABSTRACT	c. THIS PAGE	UU	36	19b. TELEPHONE NUMBER (Include area code)
Unclassified	Unclassified	Unclassified			410-306-0811

Standard Form 298 (Rev. 8/98)
Prescribed by ANSI Std. Z39.18

Contents

List of Figures

1. Introduction

Combustion synthesis offers an attractive alternative route for the preparation of intermetallics (*1*). Two different reaction modes are possible in combustion synthesis: self-propagating high-temperature synthesis (SHS) and thermal explosion (*2*). The SHS reaction mode is achieved by local heating of reactants by an external heat source and is possible only when the exothermic enthalpy of formation for the desired intermetallic product is relatively large, such as those of nickel aluminides or platinum aluminides (*3*, *4*). In contrast, for the thermal explosion mode the reactants are heated simultaneously—for example, in a furnace—until the reaction takes place over the entire sample. The final product often contains secondary product phases due to diffusion during the heating process prior to the onset of the combustion reaction (*5*).

Combustion synthesis can be achieved both in mixed reactant powder compacts and in fully dense multilayer materials (*6*, *7*). The reactant powders are usually pressed into a pellet of certain green density to conduct the combustion synthesis process. Typically, multilayered systems are fabricated by physical vapor deposition (PVD), such as magnetron sputtering or electron-beam evaporation. These methods involve creating a vapor of each element, known as the source materials, and then, in an alternating manner, depositing the vapors onto a substrate. The rate at which the vapor is deposited is controllable, allowing the growth of multilayer films with thickness ranging from nanometers to micrometers. Alternatively, multilayer foils can also be made by cold rolling (*8*–*11*). The advantages of the cold-rolling method are its simplicity, low cost, and time-efficient nature compared with PVD methods.

Over the last decade, exothermic formation reactions have been reported to self-propagate in a variety of reactive systems, such as Ni/Al, Ti/Al, or Nb/Si multilayered foils (*3*, *7*, *12*). These materials consist of alternating layers of reactants with a large negative enthalpy of mixing. The SHS reaction in these multilayers is driven by a reduction in chemical bond energy. The local reduction of chemical bond energy produces a large quantity of heat that is conducted down the multilayers and facilitates further atomic mixing and compound formation. If atomic mixing and energy release occur sufficiently fast compared to heat losses, then the reactions are self-sustaining. SHS reactions can be initiated in these multilayers at room temperature with a small thermal pulse. Such exothermic reactions in multilayers can be used as local heat sources to melt solders or brazes and thus join components in a variety of applications, such as making stainless steel-stainless steel, Al-Al, Ti-Ti, SiC-Ti, Si-Si, and bulk metallic glass (BMG)-BMG joints (*13*–*19*).

Previous literature usually treats the SHS and thermal explosion modes of combustion synthesis separately. Rabinovich et al. (*20*) analyzed the conditions for combustion synthesis in Ni/Al nanofilms and summarized several parameters, such as the number of bilayers and heating rates that can affect the reaction modes of the films. Anselmi-Tamburini and Munir (*21*) studied the

SHS reaction in laminated Ni/Al foils and established a sequence of reactions between the two metals. To the authors' knowledge, it has not been reported that both modes of reaction can occur sequentially in a single multilayer sample. That is, these two reaction modes can only be achieved in different samples with different ignition conditions. However, in the cold-rolled Ni/Al multilayer foils studied in this report, both thermal explosion and SHS reaction modes occurred sequentially after ignition.

Reactions in the Ni/Al multilayer system have been extensively investigated both theoretically and experimentally. In PVD multilayers, Ma et al. (*22*) performed calorimetric measurements on Ni/Al multilayer films prepared by electron-beam evaporation. It was demonstrated that under controlled annealing conditions, the formation of the single Al_3Ni product phase took place in two stages. The first stage is the nucleation, growth, and formation of a continuous layer, kinetically separated from the one-dimensional thickening growth stage, resulting in two separate calorimetric peaks (*22*). Similar results were also obtained by Barmak et al. (*23*) using sputtered Ni/Al multilayer films. Ma et al. (*22*) attempted to investigate the processes preceding Al_3Ni formation and found that the Ni and Al composition profiles broadened upon annealing to a stage prior to Al_3Ni nucleation, indicating that interdiffusion had taken place. They interpreted that the interdiffused region was mainly composed of solid solutions. Edelstein et al. (*24*) found that in Ni/Al multilayer films prepared by ion beam deposition, the first phase to form can be AlNi, Al_3Ni, or Al_9Ni_2, depending on the overall stoichiometry and the modulation period of the multilayers. Barmak and coworkers (*23*) found that B2 AlNi phase and an amorphous phase were formed during deposition of the multilayers made by magnetron sputtering, which considerably reduced the driving force for subsequent reactions. Depending on the periodicity of the multilayers, the formation of Al_3Ni or Al_9Ni_2 followed by Al_3Ni was observed in their study. In the work of Blobaum et al. (*25*), Al_9Ni_2 was the first phase to form in a series of Ni/Al multilayers except for a very small bilayer period (12.5 nm), where Al_3Ni was the first phase observed.

In contrast to the PVD foils, in the cold-rolled Ni/Al multilayer foils Sieber et al. (*8*), Qiu and Wang (*9*), and Battezzati et al. (*10*) all demonstrated that the first detectable phase to form was Al_3Ni. However, more recently, work done by Sauvage et al. (*26*) on cold-rolled Ni/Al multilayers revealed that a severe deformation process can induce metastable or nonequilibrium solid solutions with various compositions prior to the formation of any new product phase.

To elucidate this reaction sequence in more detail, the entire reaction process in the cold-rolled Ni/Al multilayer foils was characterized. Additionally, another cold-rolled multilayer system, Ti/Al, was also investigated, and the different reaction behaviors of these two systems are compared.

2. Experimental Procedures

The Ni/Al multilayer foils were fabricated by a cold-rolling method using a laboratory rolling mill with a roller diameter of 65 mm. Figure 1 shows the schematic of the cold-rolling procedure. Thin sheets of pure elements of Ni and Al with initial thickness of 25.4 and 38.1 μm, respectively,[*] were alternatively stacked together in order to obtain a 1:1 atomic ratio (2:3 thickness ratio) of Ni/Al (figures 1a and b). The stacked sheets were then rolled to form a tube (figure 1c). Two tubes were made at the same time with the same number of Ni/Al layers. Ni was the outer layer for one tube, and Al was the outer layer for the other tube. These two tubes were flattened by a vise, placed in a folded stainless-steel sheet that had been previously hardened by repeated rolling, and cold rolled a few times to reduce the thickness to half of their original thickness (figure 1d). Afterward, they were taken out of the stainless-steel sheet and stacked together to recover the original thickness. In this way, two of the same metal layers would not become layered side by side in the final multilayer foil. The stacked foils were then cold rolled without changing the distance between the rollers. The thickness of the foil was reduced to half in one rolling pass. Subsequently, the resulting foils were cut into halves and stacked together, and the rolling procedure just mentioned was repeated for several times until a uniform multilayer foil was achieved (figures 1e, f, and g). The total thickness of the foil was ~200 µm. Further details of the cold-rolling process are described elsewhere (*27*).

Ti/Al multilayer foils were also fabricated using a similar cold-rolling procedure. Thin sheets of pure elements of Ti and Al with initial thickness of 32 and 38.1 μm, respectively,[†] were stacked alternatively together in order to obtain a 1:1 atomic ratio of Ti/Al. Making homogeneous Ti/Al multilayer foils was difficult because Ti is much harder than Ni and, as a result, it is difficult to deform Ti during the rolling process. Therefore, the resulting foils fell apart easily. Consequently, in order to fabricate uniform Ti/Al foils, the Ti sheets were first annealed at 700 °C for 2 h in an Ar atmosphere prior to rolling. In this way, it was possible to obtain homogeneous Ti/Al multilayer foils that were fabricated with a total thickness of 260 µm.

SHS reactions in the cold-rolled Ni/Al multilayer foils were initiated by heating one end of the foils in a flame with a temperature around 500 °C in air for several seconds. The reaction velocities were measured under such conditions using a digital camcorder with a temporal resolution of 0.03 s. The dimensions of the foils were $0.2 \times 0.5 \times 2.5$ mm. To characterize the reaction products, the reacted Ni/Al foils were ground into powders for symmetric x-ray

---

[*]Ni minimum purity of 99.6 weight-percent and Al minimum purity of 99 weight-percent (McMaster-Carr Supply Company, Princeton, NJ).

[†]Ti minimum purity of 99.6 weight-percent (Alfa Aesar, Ward Hill, NY) and Al minimum purity of 99 weight-percent (McMaster-Carr Supply Company, Princeton, NJ).
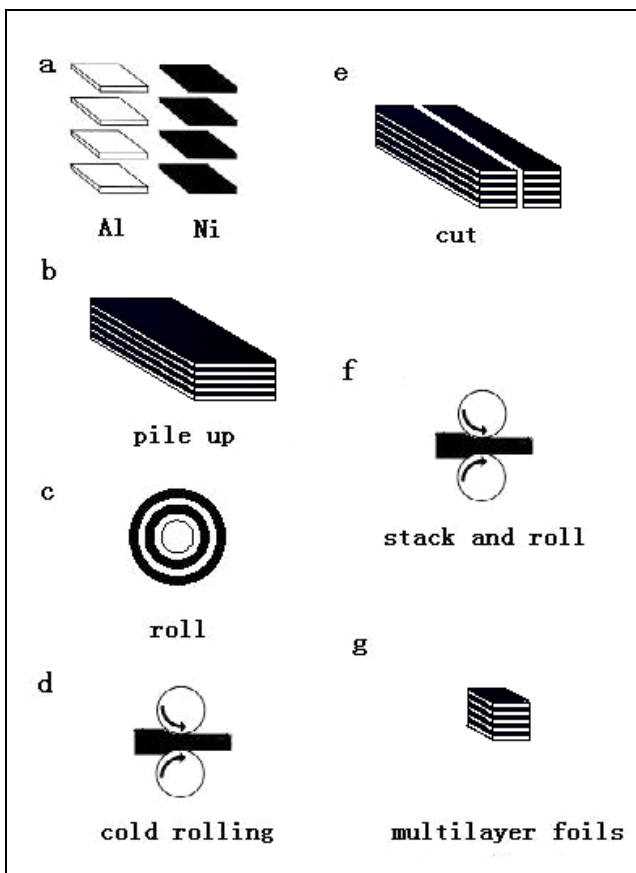
Figure 1. Schematic of the cold-rolling procedure.

diffraction (XRD) examination using Cu Kα radiation. The unreacted as-cold-rolled Ni/Al foils were also examined for comparison.

Cross sections of as-cold-rolled and reacted foils were polished, examined, and characterized using a Hitachi S-3600N scanning electron microscope (SEM) equipped with energy dispersive x-ray analysis (EDX) capability. The reacted foil was etched by electropolishing to reveal the post-reaction equilibrium grain size and grain boundaries, where the reacted foil was used as the anode and a graphite bar was used as the cathode. The electrolyte was a mixture of 80% acetic acid and 70% perchloric acid with a volume ratio of 9:1. The electropolishing process was conducted under 20 V at room temperature for 10 min.

The evolution of heat from the reaction process of the as-cold-rolled foil was measured using a Perkin-Elmer differential scanning calorimeter (DSC). In each DSC run, about 10 mg of multilayer foil was heated from 50 to 725 °C at a rate of 40 °C/min in flowing N_2. Because at 725 °C the reaction was still not entirely completed, additional DSC runs were performed to 1000 °C to ensure all reactants were consumed. A baseline was obtained by repeating the heating cycle, which was then subtracted from the heat flow data obtained in the first run. By integrating the net heat flow with respect to time, the heat of reaction could be obtained. Ni/Al

multilayer foils made by magnetron sputtering (total foil thickness 40 μm and bilayer thickness 70 nm)[*] were also examined by XRD and DSC for comparison. However, because the PVD Ni/Al foils were made by magnetron sputtering, the Ni layers contained about 7 weight-percent V, an alloying element in the Ni sputter source. Therefore, it was expected that the presence of V would lower the total heat output from the PVD foil. As such, integrated total energy would be somewhat less.

3. Results and Discussion

3.1 Thermodynamic Assessments of the Ni-Al and Ti-Al Equilibrium Phase Diagrams

As shown in figure 2, the Ni-Al system consists of the five equilibrium intermetallic phases of Al_3Ni, Al_3Ni_2, AlNi, Al_3Ni_5, and $AlNi_3$ (*28*, pp 181–184). Whereas the Al_3Ni phase is a line compound, the other intermetallics are stable for a range of Al:Ni ratios; Al_3Ni_2 is stable for Ni contents from 36.8 to 40.5 atomic percent (at.%) Ni; the congruently melting AlNi is stable for Ni contents from 42 to 69.2 at.% Ni; Al_3Ni_5 is stable for Ni contents from 64 to 68 at.% Ni; and $AlNi_3$ is stable for Ni contents from 73 to 76 at.% Ni. There are two eutectic reactions at 2.7 (L ↔ Al_3Ni + Al) and 75 at.% Ni (L ↔ Ni + $AlNi_3$), respectively; three peritectic reactions at 15 (L + Al_3Ni_2 ↔ Al_3Ni), 26.9 (L + AlNi ↔ Al_3Ni_2), and 74.5 at.% Ni (AlNi + $AlNi_3$ ↔ Al_3Ni_5); and a peritectoid reaction (AlNi + $AlNi_3$ ↔ Al_3Ni_5) at 60.5 at.% Ni (*28*, pp 181–184).
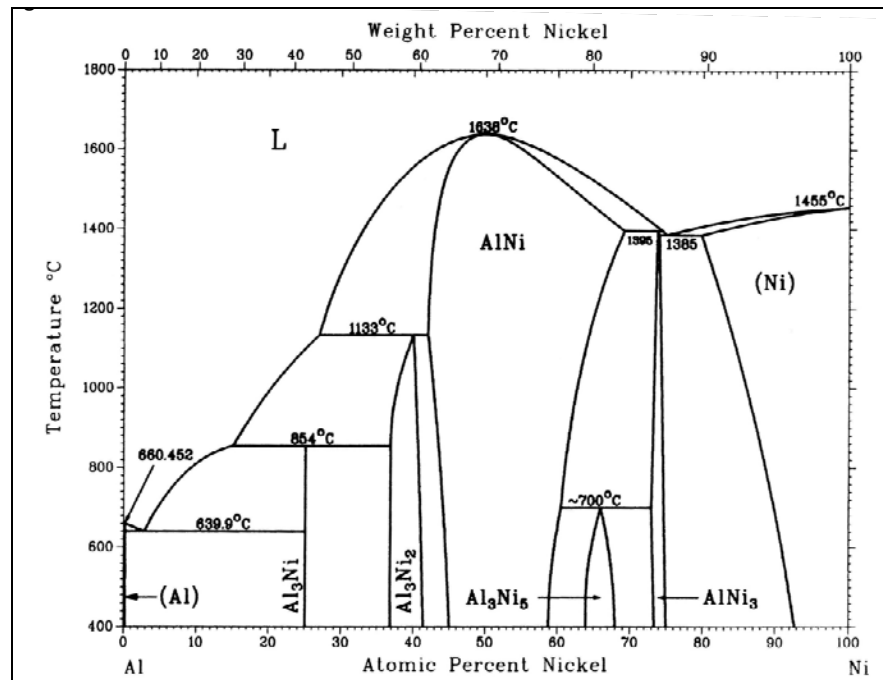
Figure 2. The Al-Ni equilibrium phase diagram.

The Ti-Al system is quite different in many respects. Figure 3 depicts that there are no eutectic reactions, and the number of intermetallic phases is greater (*28,* pp 225–227). The allotropic transformation from hcp αTi to bcc βTi complicates the potential transformations. The equilibrium intermetallic phases consist of $TiAl_3$, $TiAl_2$, TiAl, and Ti_3Al. Additionally, there are several other phases, such as the nonequilibrium phase of Ti_3Al_5 and long-period superlattice structure δ and tetragonal superlattice structure $\alpha TiAl_2$, associated with the $TiAl_3$ equilibrium structure. Again, the $TiAl_3$ phase is a line compound. The other intermetallics are stable for a range of Ti:Al ratios: $TiAl_2$ is stable for Al contents from 65 to 68 at.%; TiAl is stable for Al contents from 48 to 69.5 at.%; and $AlTi_3$ is stable for Al contents from 22 to 39 at.%. There are two eutectoid reactions at 40 (αTi $\leftrightarrow$ Ti_3Al + TiAl) and 71.5 at.% Al (δ $\leftrightarrow$ $TiAl_2$ + $TiAl_3$), respectively; four peritectic reactions at 53 (L + βTi $\leftrightarrow$ TiAl), 73.5 (L + TiAl $\leftrightarrow$ δ), 80 (L + δ $\leftrightarrow$ $TiAl_3$), and 99.9 at.% Al (L + $TiAl_3$ $\leftrightarrow$ Al); and two peritectoid reactions (βTi + TiAl $\leftrightarrow$ αTi) at 43 and (TiAl + δ $\leftrightarrow$ $TiAl_2$) 65 at.% Al.
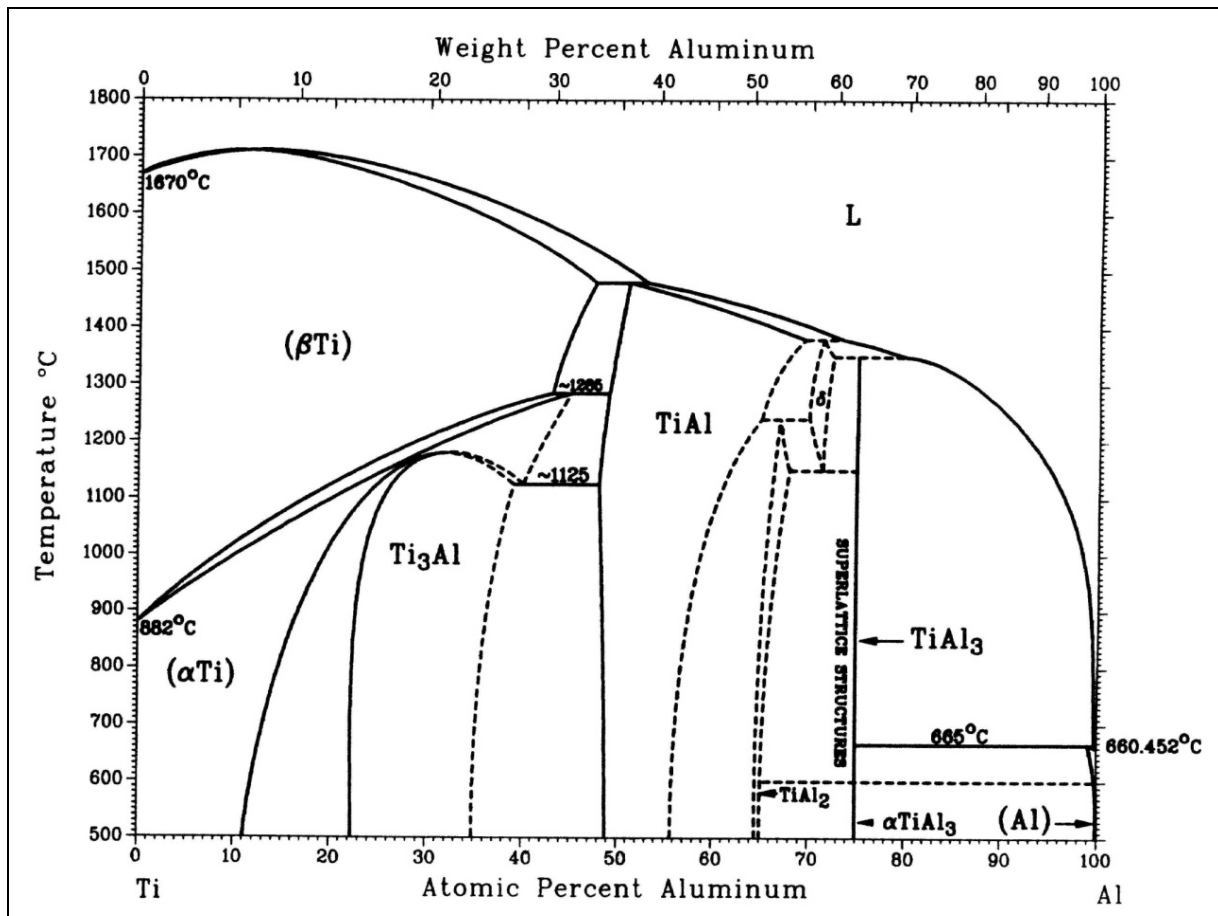

Figure 3. The Al-Ti equilibrium phase diagram.

3.2 Ni-Al Multilayer System

To establish the nature and identity of the reaction product from the first stage, foils removed from the flame after completing the first stage of the reaction process were compared to those allowed to complete both stages. Further differences in the phase evolution in the two types of foils were studied by DSC using a slow and controlled method to heat the samples. Multiple exotherms could be identified for both types of foils. Using DSC, both the as-cold-rolled and partially reacted foils were heated to each peak temperature to identify the reaction product associated with each exothermic peak. XRD and SEM analyses showed that the first two peaks corresponded to the formation of Al_3Ni, while the third peak corresponded to the formation of AlNi.

3.2.1 Characterization of the SHS-Reacted Cold-Rolled and PVD Ni-Al Foils

Combustion synthesis reactions started in the cold-rolled Ni/Al foil after heating one end of the foil in a flame for several seconds. Three reaction stages were identified during the synthesis process. Figure 4 displays typical snapshots from each of the three stages of the process. In stage one, the reaction spread along the direction parallel to the surface of the foil at a relatively slow rate. The morphology of the surface of the foil changed, and the otherwise bright, shiny surface reflectivity of the foil was lost, and the surface became dark and dull. The darkening is most likely associated with the formation of surface oxides or nitrides of the precursor Al or Ni. As such, the motion of the reaction front was easily observed visually. The propagation front velocity for the cold-rolled Ni/Al multilayer foils in the first reaction stage was measured to be around 7 mm/s. A similar phenomenon has been observed by Myagkov et al. ([29]) in two-layer thin films of Ni/Al. The measured propagation velocity of the reaction front in their study was around 5 mm/s. According to Rabinovich et al. ([20]), this reaction wave can be interpreted as a displacement of the reaction zone only. This is because the measured velocity was not higher than several centimeters per second. The expected characteristic velocity of an SHS propagation wave in multilayer thin films should be about several meters per seconds ([30], [31]). At lower wave propagation velocities, the heat losses will extinguish the self-propagating combustion. From the previous discussion, the first reaction stage of the combustion synthesis in cold-rolled Ni/Al multilayer foils can be identified as a displacement of the reaction zone that follows a displacement of the nonuniform heating within of the sample. That is, the displacement of the reaction zone corresponds to a traveling heat wave through the specimen causing a limited or partial conversion of reactants to products.

Then, in stage two, the part of the foil that was in the flame experienced thermal explosion. During this part of the process, the foil released a large amount of heat, emitting visible red light. The heat release triggered a self-propagating reaction traveling across the entire foil with great velocity, which was defined as the third stage of combustion synthesis in the cold-rolled Ni/Al multilayer foils. Recall in figure 4 the snapshots illustrating the reaction process of a cold-rolled Ni/Al multilayer foil recorded by a digital camcorder.
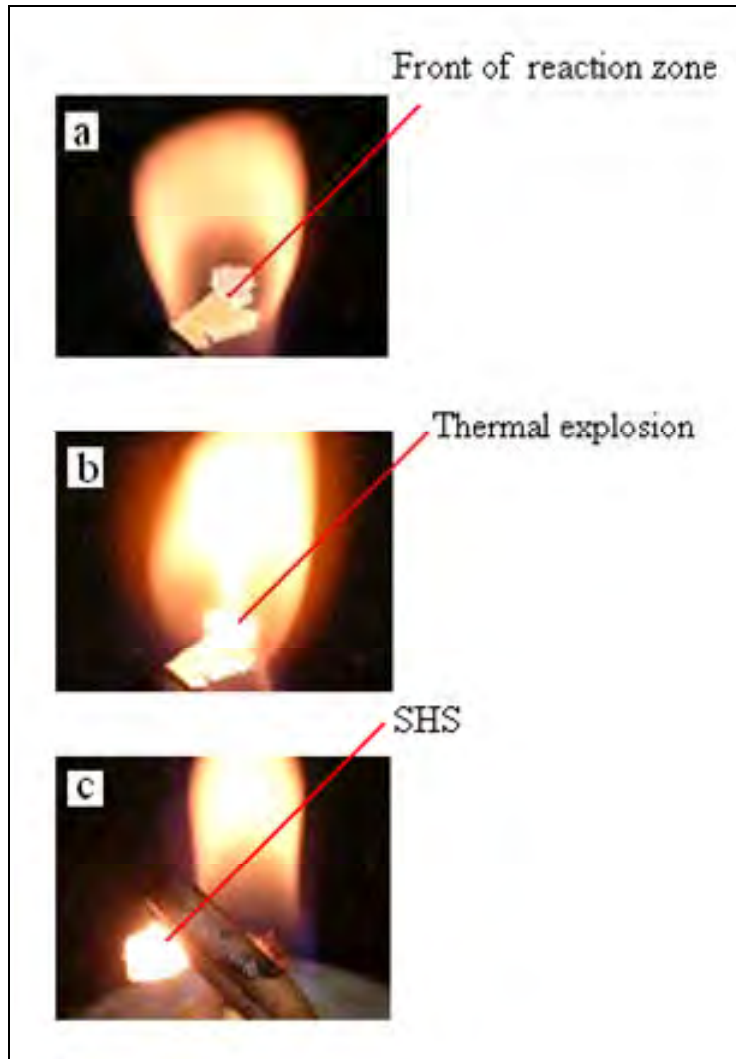
Figure 4. Combustion synthesis process of the cold-rolled Ni/Al
multilayer foils: (a) reaction front of the displacement
of the reaction zone, (b) thermal explosion occurring in
the part of the foil that was put in the flame, and (c) the
SHS reaction.

Figures 5a and b show the XRD trace of an unreacted cold-rolled multilayer foil and its final reaction product. Likewise, figures 6a and b show the XRD trace of an unreacted PVD multilayer foil and its final reaction product. The trace for the PVD foil contains only four Bragg reflection peaks, namely for Al (111) and (222), and for Ni (111) and (222). The trace for the unreacted as-cold-rolled foil contains most of the Ni and Al crystal orientation reflections. In contrast, the traces for the reaction products from both the cold-rolled and the PVD foils are very similar, which were identified as the ordered B2-type AlNi compound. Since the reacted cold-rolled foils and PVD foils were ground into powders for XRD examination, no texture could be observed in the reaction products.
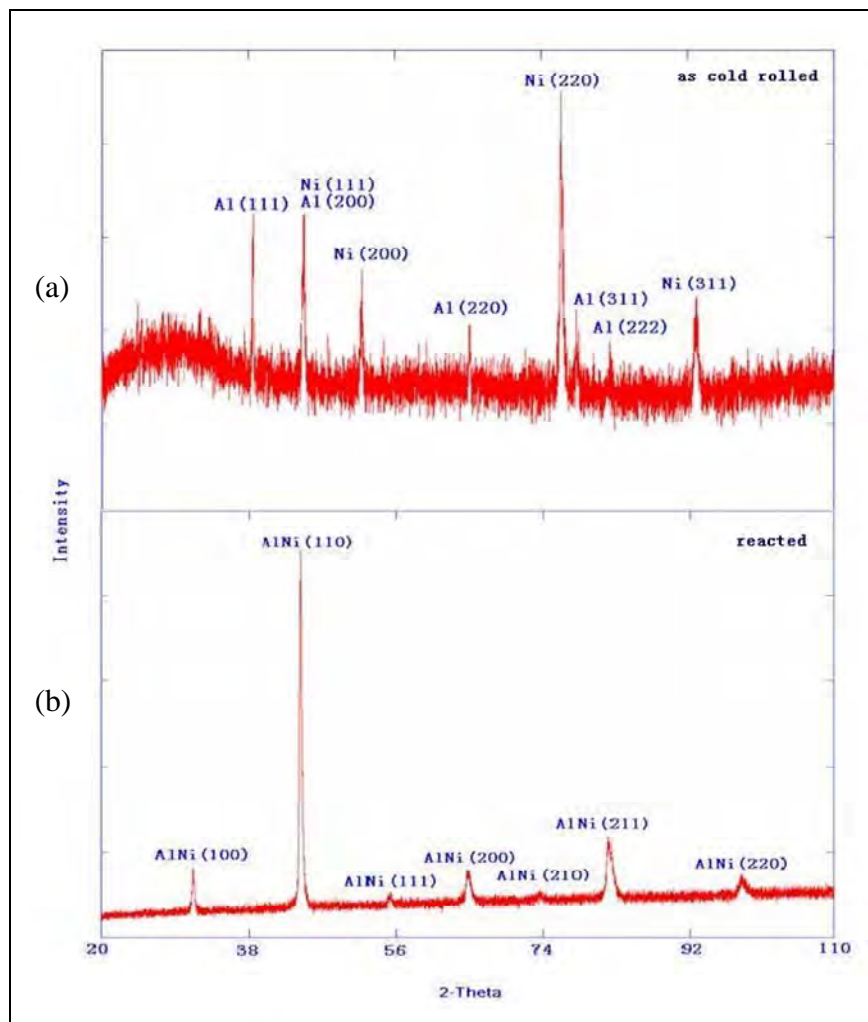
Figure 5. XRD patterns of (a) an as-cold-rolled Ni/Al multilayer foil and (b) its reaction product.
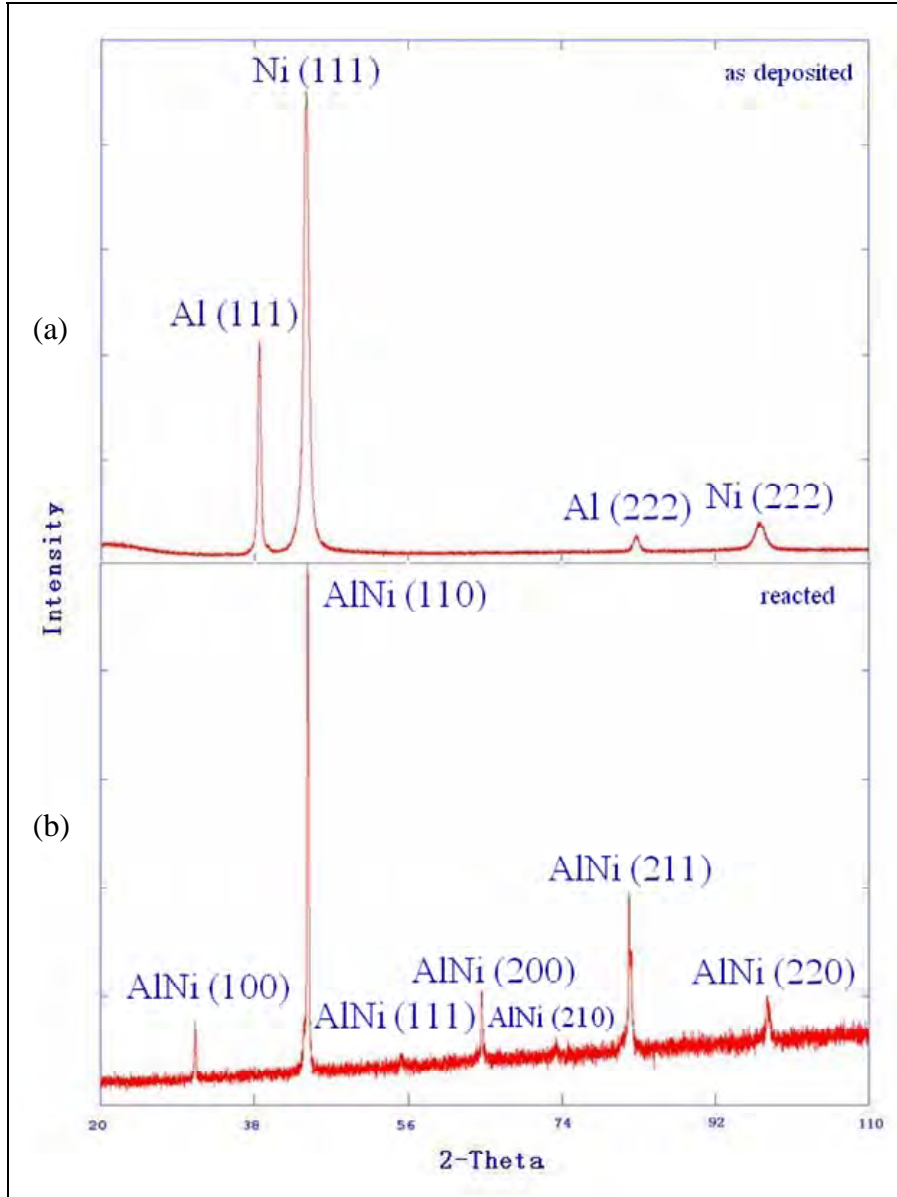
Figure 6. XRD patterns of (a) a PVD foil and (b) its SHS-reacted reaction product.

Figure 7a and b shows SEM images of both the as-cold-rolled and reacted Ni/Al foils. In the as-cold-rolled Ni/Al multilayer foils, no sign of reaction can be observed. Typically, in the as-cold-rolled Ni/Al multilayer foils, necked Ni particles are embedded in the Al matrix and aligned along the rolling direction (see figure 7a). Most of the Ni particles possess a wavy irregular surface. The average bilayer thickness of the as-cold-rolled foils is around 10 µm, which is much thicker than those found in most PVD foils. In comparison, the PVD foils typically have bilayer thicknesses in the range of tens of nanometers (7).
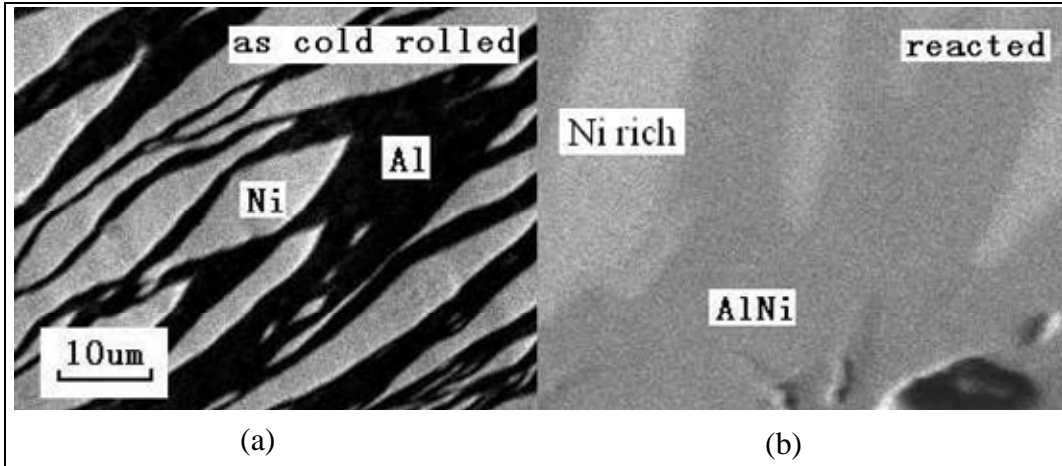
Figure 7. SEM images of an as-cold-rolled Ni/Al multilayer foil and its reaction product.

According to Sauvage et al. (*26*), in cold-rolled Ni/Al multilayer foils, intermixing induced by plastic deformation was observed only in the regions of samples where the bilayer thickness was below 10 nm. In our cold-rolled samples (with a bilayer thickness around 10 µm), almost no intermixing can be observed at the Ni/Al interface.

As shown in figure 7b, two phases can be observed and identified in the reacted cold-rolled foil: the primary reaction product, AlNi, and some Ni-rich phase. Although there is some backscattered electron contrast between the AlNi phase and the Ni-rich phase, the amount of the Ni-rich phase is very limited and therefore could not be identified with XRD (see figure 5). Because the AlNi phase field is stable for a wide range of Ni contents (42–67 at %), it is surmised that this contrast is most likely associated with an Ni-rich variant of AlNi. There are also some pores in the reacted foil, which arise from contraction during rapid cooling and concomitant density increase during the reaction. Figure 8 shows an SEM image of a reacted cold-rolled Ni/Al foil after electropolishing. The average AlNi grain size was estimated to be around 15 µm. The lack of the Ni-rich phase on the sample surface might be due to a faster etching rate of the Ni-rich phase than that of AlNi during electropolishing.

The measured reaction velocities for the first reaction stage were around 7 mm/s for five pieces of foils, which was much slower than the reaction speed in the Ni/Al multilayer foils made by PVD methods that have reaction velocities ranging between 1 and 30 m/s (*30*, *31*). The lower speed in the cold-rolled foils was due to the much larger Ni/Al bilayer thickness. As the bilayer thickness becomes larger, the atomic diffusion distances are longer and, therefore, atoms mix more slowly. As such, heat is released at a lower rate, and the reactions travel more slowly through the foil. In addition, the alternating Ni/Al layers in the cold-rolled foil were not uniform, thus making it difficult to ignite the foil and reduce the speed of the self-propagating reaction.
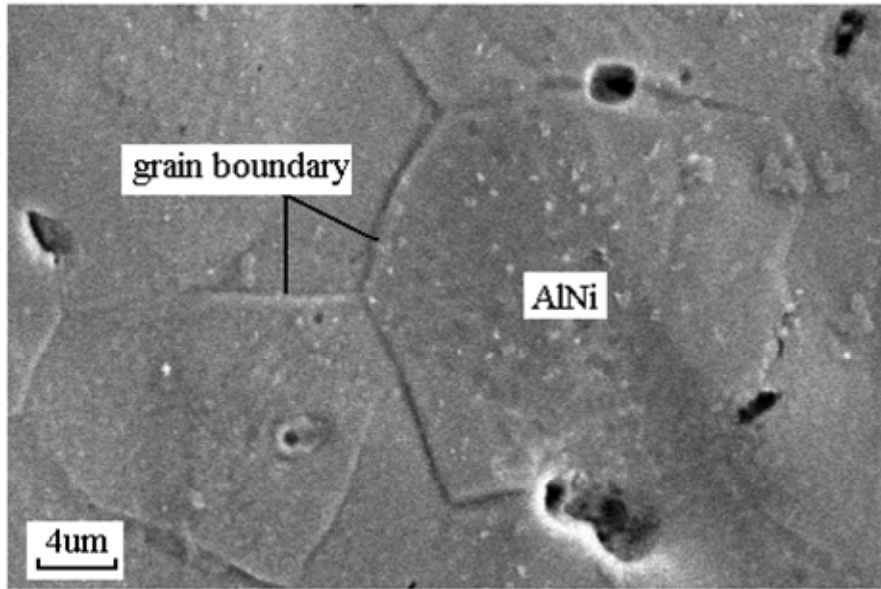
Figure 8. SEM image of a cold-rolled Ni/Al foil after complete SHS reaction and electropolishing.

Despite such shortcomings in the cold-rolled multilayer foils, this method's ease of fabrication, low cost, and time efficiency made it advantageous. Meanwhile, the reduction in reaction velocity also made the cold-rolled foil an ideal system to study the details of the formation reactions in multilayer foils.

To further elucidate and identify the phase evolution during the displacement phase of the reaction zone, some Ni/Al multilayer foils were taken out of the flame to terminate the first stage of the reaction in the middle of the foil. Figure 9 shows the SEM image of the reaction front of such a foil. A thin layer of Al-rich phase (Al_3Ni, the Ni/Al atomic ratio obtained by EDX is approximately 1:3) can be seen to have grown around the necked Ni particles. Such Al-rich layers were continuous at the Ni/Al interface and fully encircled the Ni particles. The SEM observation suggests that in the combustion synthesis of cold-rolled Ni/Al multilayer foils, the first reaction stage is the formation of a continuous Al_3Ni layer around the Ni particles.

The entire reaction process for the cold-rolled Ni/Al multilayer foils in combustion synthesis can be identified as follows: The first reaction stage is a displacement of the reaction zone with Al_3Ni as the reaction product ($Ni + 3Al \rightarrow Al_3Ni$). Then, the part of the foil in the flame goes through a thermal explosion reaction. The heat released by this reaction triggers the SHS reaction across the foil and results in the formation of the final reaction product AlNi.

3.2.2 Characterization of the DSC-Reacted Cold-Rolled and PVD Foils

As shown in figure 10, the DSC thermogram of the as-cold-rolled Ni/Al multilayer foil reveals the convolution of three peaks. The very large broad peak, centered on position C, contains a superimposed peak appearing as a shoulder (position A) and a sharp peak (position B). For
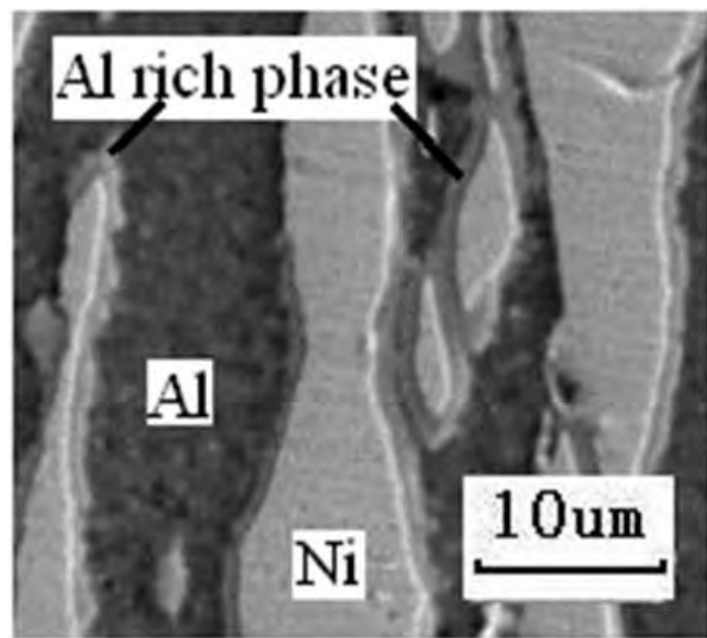
Figure 9. SEM image of the reaction front of a quenched Ni/Al
multilayer foil.
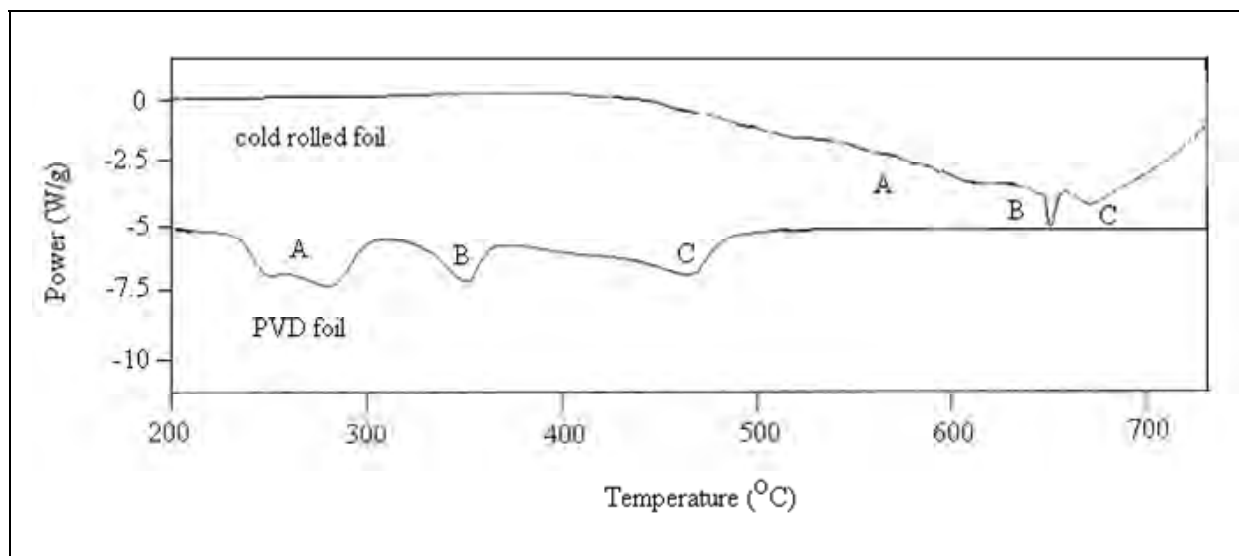
Figure 10. DSC curves for an as-cold-rolled Ni/Al multilayer foil and an as-deposited PVD Ni/Al multilayer foil.

comparison, the DSC thermogram for a PVD foil with a bilayer thickness of 70 nm is also included in the figure. There are three well-separated peaks in the latter curve; actually, the lowest temperature peak is a superposition of two peaks.

The differences between the peak shapes of the two types of DSC curves are indicative of different underlying reaction mechanisms. First, the peak temperatures for the cold-rolled foil are much higher than those for the PVD foil. This is due to the much larger bilayer thickness (around 10 µm for the cold-rolled foils vs. tens of nanometers for the PVD foils) and the nonuniform structure of the cold-rolled foils. Second, while the peak positions identified by the letters in the cold-rolled foil are well separated along the temperature axis, they are on top of a very large, broad "feature" that seems to dominate the entire thermal process. Third, the peak profiles in the two foil types are not the same. Last, notable differences in the relative peak amplitudes are reflective of the extent of contributions (both heat output and phase formation) to the overall reaction sequence.

To identify the evolution of reaction products from the different reaction stages for the cold-rolled Ni/Al multilayer foils, some of the as-cold-rolled foils were heated to 350 °C (slightly below the onset temperature of the shoulder peak A in the DSC trace), 530 °C (the midpoint temperature of peak A), 640 °C (the midpoint temperature of peak B), and 725 °C (the maximum temperature for the DSC scans) using the same heating rate as in the previous DSC runs. Figure 11 shows the XRD pattern and SEM image for the cold-rolled foil heated to 350 °C. They are similar to those for the as-cold-rolled foils. Only Ni and Al can be identified in the annealed foil.

For the as-cold-rolled foil heated to 530 and 640 °C (figures 12a and b), Al_3Ni peaks appear among the Ni and Al peaks, suggesting that Al_3Ni was generated at these temperatures. For the foil annealed to 530 °C, Al_3Ni layers can be observed at isolated sites along the Ni/Al interface. The inset in figure 12a suggests that position A in the DSC curve is associated with the growth of Al_3Ni at isolated nucleation sites. In the foil annealed to 640 °C, the Al_3Ni layers are continuous, fully covering the Ni particles. Also, growth in thickness along the direction normal to the surface toward neighboring Ni particles can be observed (see figure 12b). This suggests that peak B in the DSC curve is related to the growth of Al_3Ni in the direction normal to the Ni/Al interface. Therefore, both DSC peak positions A and B in the curve of the cold-rolled Ni/Al multilayer foils are associated with the exothermic formation of Al_3Ni. This is in agreement with earlier qualitative interpretations of the two exothermic DSC peaks that were observed for the formation of a single phase (*22*, *32*). However, in Ma et al.'s (*22*) and Coffey et al.'s (*32*) models, it was assumed that the generation of Al_3Ni occurred as a two-stage process in reactive foils where the reactant interspacing was significantly reduced. The first step was the lateral growth of the Al_3Ni phase from isolated nucleation sites and the subsequent coalescence into a continuous layer. The second step was the growth of such Al_3Ni layers in the direction normal to the interface until all Al was consumed.

14
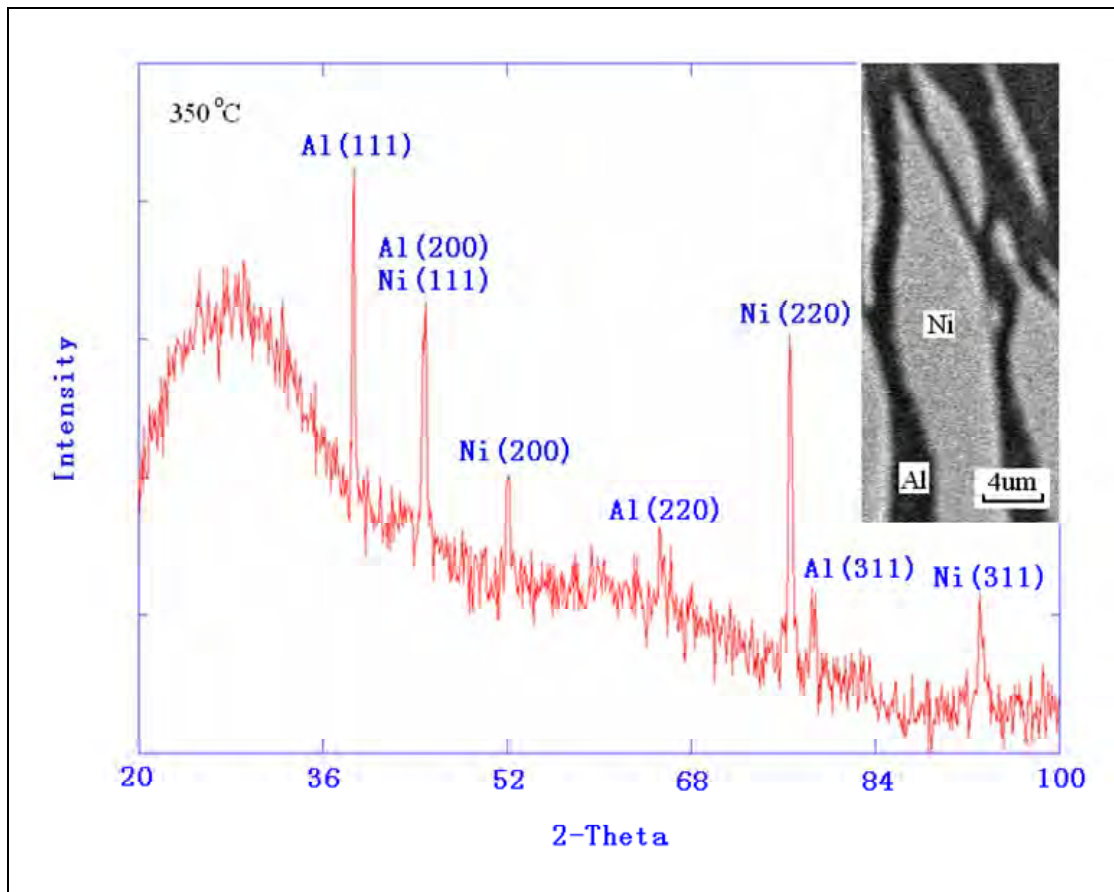
Figure 11. XRD pattern and SEM image for the as-cold-rolled Ni/Al multilayer foils heated to 350 °C in the DSC.
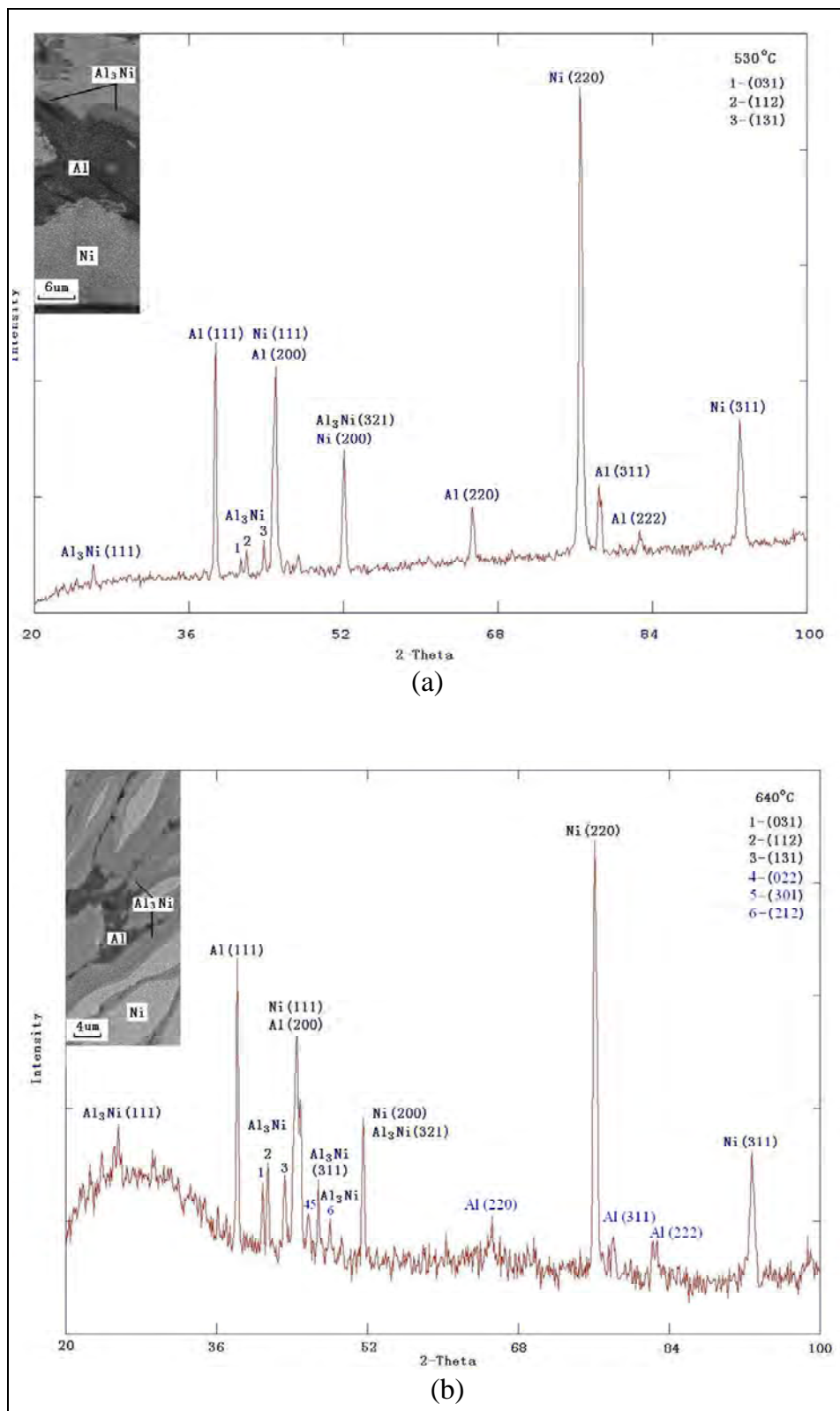
Figure 12. (a) XRD pattern and SEM image for the as-cold-rolled Ni/Al multilayer foils heated to 530 °C in the DSC. (b) XRD pattern and SEM images for the as-cold-rolled Ni/Al multilayer foils heated to 640 °C in the DSC.

Our XRD and SEM results do not precisely support Coffey's model for the two-stage formation process of Al_3Ni. Specifically, the size and shape of peaks A and B (see figure 10) do not match Coffey's model. It is likely that such an extrapolation to a greater separation of the reactants manifested in the cold-rolled foils cannot be made. Instead, reactions in the cold-rolled foils might be governed by another mechanism that is described as follows.

In the DSC curve for the cold-rolled foils, the first peak is broad and the second peak is narrower and very small; this is partially due to the nonuniform interfacial area. The triangular shape of peak A is consistent with a diffusion-controlled process. There is a definite change in the growth mode of the Al_3Ni layer, as indicated by the appearance of peak B. For the as-cold-rolled foils heated to 725 °C (figure 13), three to four phases can be identified: the intermediate reaction product Al_3Ni, an Ni-rich phase, unreacted Ni, and the final reaction product, AlNi; peak C in the DSC curve must be associated with the formation of the final product, AlNi. It is interesting to point out that at 725 °C, there is still a considerable amount of Ni in the foil. Note, however, that there might be some other intermetallic phases, such as Al_3Ni_2, during the transition from Al_3Ni to AlNi that require further investigation in the future.
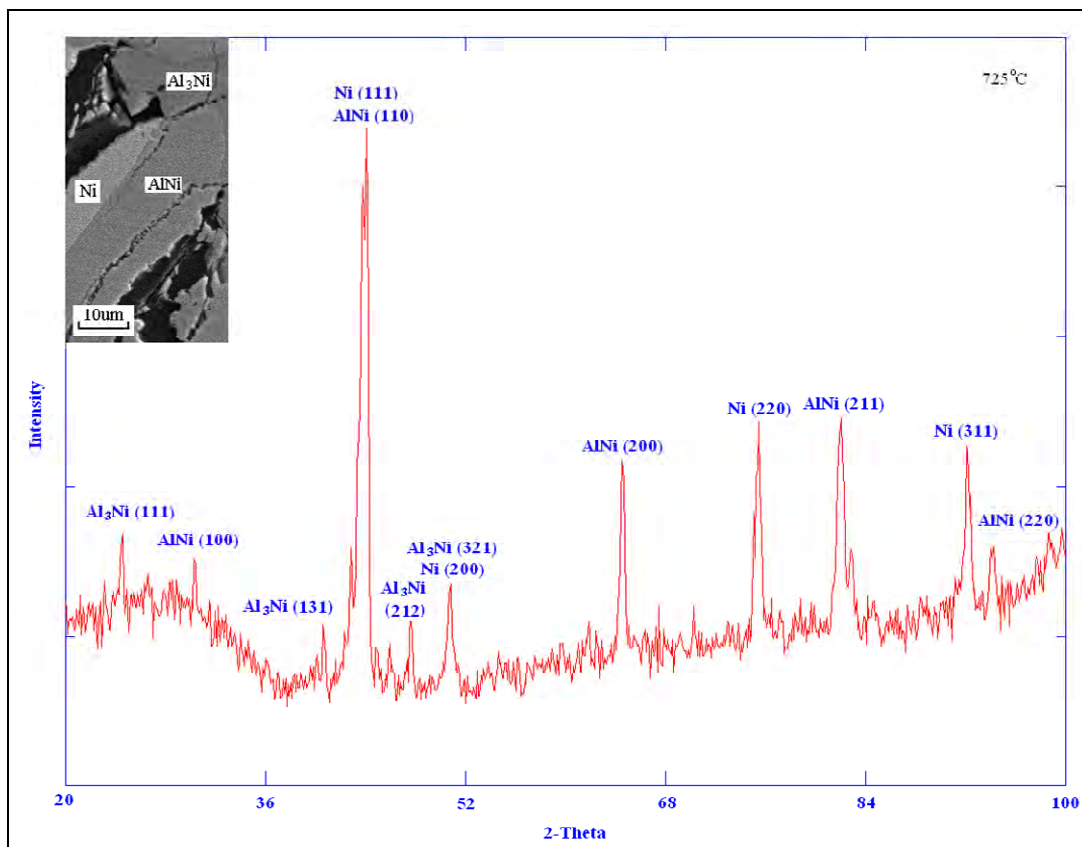

Figure 13. XRD pattern and SEM image for the as-cold-rolled Ni/Al multilayer foils heated to 725 °C in the DSC.

17

By integrating the net heat flow with respect to time of the DSC data up to 1000 °C (not shown), the heats of reactions for the cold-rolled and the PVD foils were calculated to be –57.5 and –57.9 kJ/mol, respectively. The calculated values carry a measurement/calculation error of about ±0.5 kJ/mol and are slightly smaller than the formation enthalpy of AlNi (–59 kJ/mol) (*33*). The slightly smaller heats of reaction might be due to several factors, such as prior intermixing that occurs during the multilayer fabrication process. For the PVD foils, the presence of V would also lower the total heat output. For the cold-rolled foil, the reaction products are not entirely AlNi but contain an Ni-rich AlNi phase; this would likewise cause a lower measured heat of reaction compared to the literature value.

After completing the first stage reaction in the self-propagating reactions, some cold-rolled foils were taken out of the flame to terminate the reaction in the middle of the foils. The XRD trace for the partially reacted foil (not shown) was similar to the trace of the as-cold-rolled foil, containing only Ni and Al peaks. The DSC curve for the partially reacted foil is shown in figure 14. Note that there are also three exothermic peaks in this DSC scan. Although XRD was not sufficiently sensitive to detect subtle differences, unlike the DSC trace shown in figure 10, the thermal rise to peak A is not as steep, and peak B is clearly preceded by a sharp endotherm.
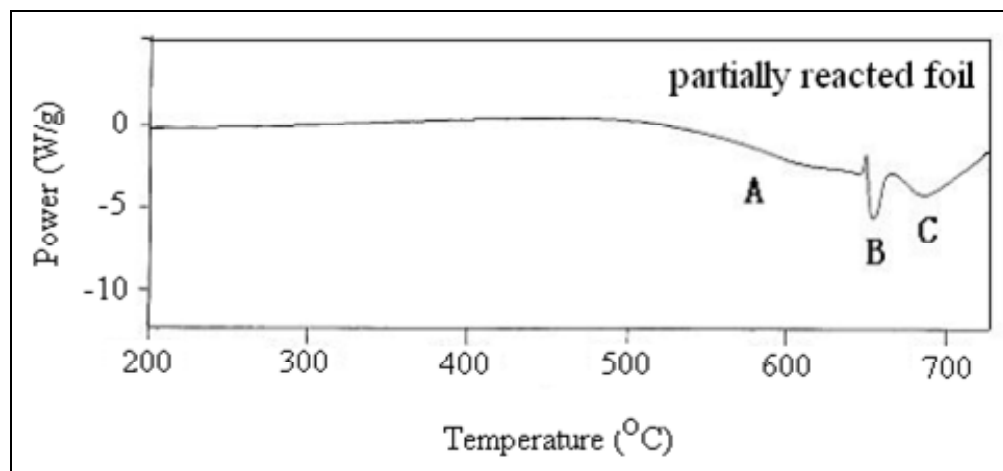
Figure 14. DSC curve for the partially reacted cold-rolled Ni/Al multilayer foil.

To identify the reaction products for the different reaction stages, some of the partially reacted foils were heated to 350 °C (below the onset temperature of peak A), 550 °C (the midpoint temperature of peak A), 660 °C (the midpoint temperature of peak B), and 725 °C (the maximum temperature for the DSC scans) using the same heating rate as in the previous DSC runs. Figure 15 shows the XRD patterns and SEM image for the partially reacted foil heated to 350 °C. The as-cold-rolled foil annealed to 350 °C only contained Ni and Al (figure 11). In contrast, in the partially reacted foil that was annealed to 350 °C, Al$_3$Ni layers (the Ni/Al atomic ratio obtained by EDX is ~1:3) can be observed at isolated sites at the Ni/Al interface. Because of the

18
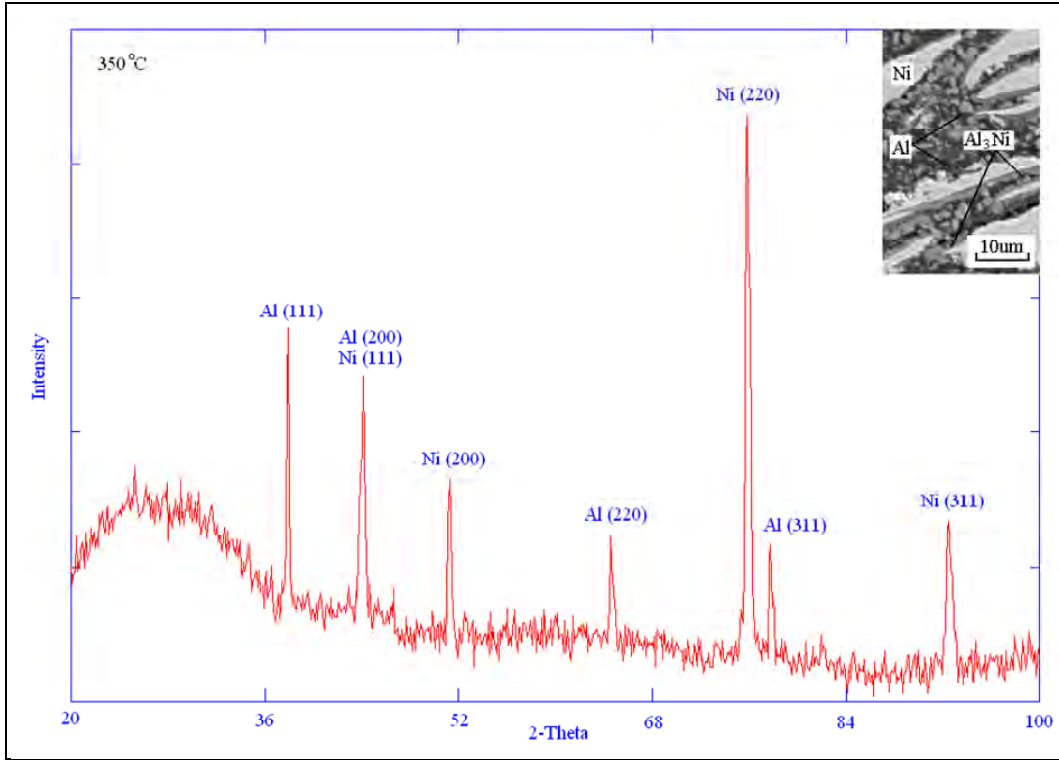
Figure 15. XRD pattern and SEM image for the partially reacted cold-rolled Ni/Al multilayer foils heated to 350 °C in the DSC.

small amount of Al_3Ni formed, it could not be identified from the XRD scan. Note that the detection limit of XRD is about 4–5 at.%. This difference between the as-cold-rolled and partially reacted cold-rolled foils confirms that the first reaction stage observed in the SHS reaction is associated with the growth of Al_3Ni at isolated nucleation sites near the Ni/Al interface.

For the partially reacted foils heated to 550 and 660 °C, the XRD traces and SEM images provide similar results to the cold-rolled foils that were heated to 530 and 640 °C. For the partially reacted foil heated to 550 °C, Al_3Ni layers appear at isolated sites along the Ni/Al interface (figure 16a), and for the partially reacted foil heated to 660 °C, the Al_3Ni layers become continuous, cover the Ni particles completely, and grow in thickness toward the neighboring Ni particles (figure 16b). Thus the first two peaks (A and B) in the DSC curve of the partially reacted Ni/Al multilayer foil could also be identified as the exothermic formation of Al_3Ni. Similar to the as-cold-rolled foils that were annealed to 725 °C, for the partially reacted foils heated to 725 °C (figure 17), there are also three to four phases in the foil: Al_3Ni, a Ni-rich phase, unreacted Ni, and the primary reaction product, AlNi. Thus peak C in the DSC scan for the partially reacted foils is associated with the formation of the final product, AlNi.
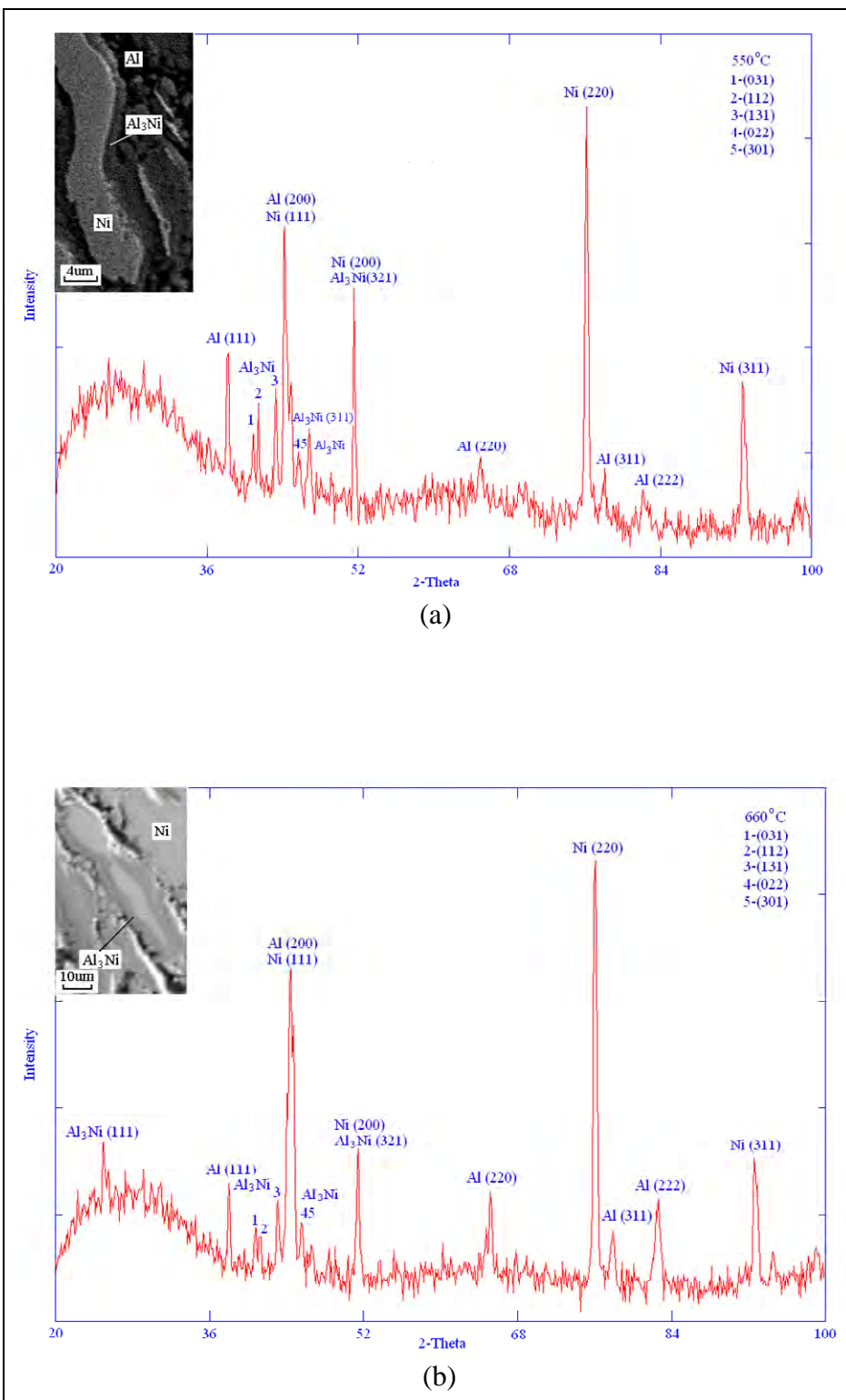
Figure 16. (a) XRD pattern and SEM image for the partially reacted cold-rolled Ni/Al
multilayer foils heated to 550 °C in the DSC. (b) XRD pattern and SEM
images for the partially reacted cold-rolled Ni/Al multilayer foils heated to
660 °C in the DSC.
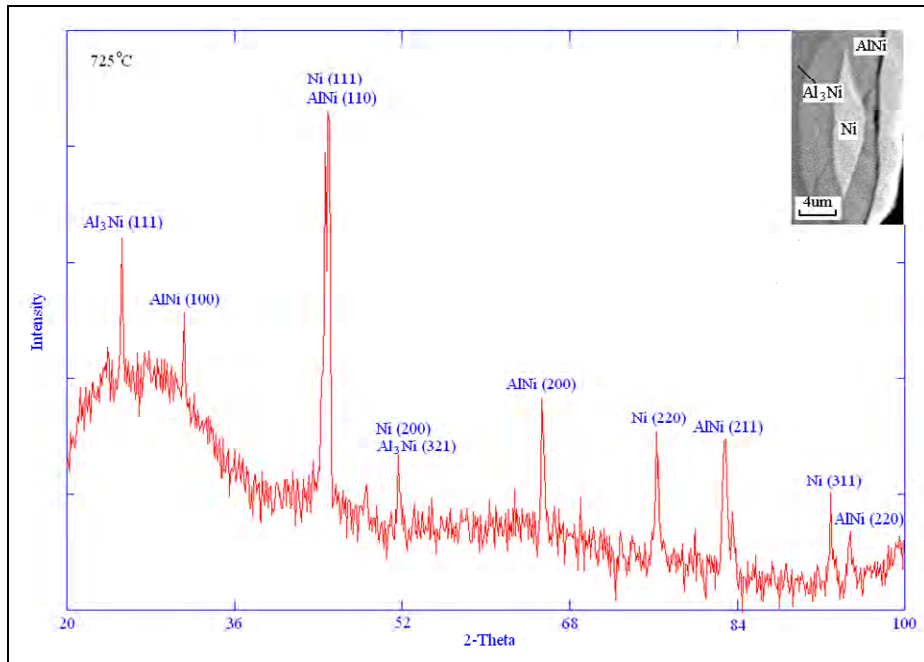
Figure 17. XRD pattern and SEM image for the partially reacted cold-rolled Ni/Al
multilayer foils heated to 725 °C in the DSC.

While there are strong similarities, there are also some differences between the DSC curves of the as-cold-rolled foil and the partially reacted cold-rolled foil. Peak A of the partially reacted foils (onset at about 500 °C) is much smaller than that of the as-cold-rolled foils (onset at about 430 °C), which suggests that the first stage of reaction has already occurred in the partially reacted foils. The diminished energy release in the DSC experiment is self-evident, as a partial conversion of the reactants to product already occurred. The transition from a diffusion-controlled to a precipitation-type mechanism is also more pronounced in the partially reacted foil with the appearance of the endothermic peak that precedes peak B. The endotherm onset appears at around 640 °C, corresponding to the melting of Al-Ni eutectic. Also, the three peak temperatures for the partially reacted foils are higher compared with the as-cold-rolled foils, indicating that more energy input from DSC is needed to complete the same phase formation process. Again, these higher peak temperatures are due to the occurrence of the first stage of the SHS reaction prior to the DSC anneal experiments in the partially reacted foils.

From data presented in the DSC curves, SEM observations, and XRD scans from both as-cold-rolled and partially reacted cold-rolled Ni/Al multilayer foils at various formation stages, some of the SHS reaction process for cold-rolled Ni/Al multilayer foils could be identified. Based on the difference between the as-cold-rolled and partially reacted foils, it may be concluded that the first reaction stage, with a slow reaction velocity, corresponds to the nucleation and growth of the Al_3Ni phase at isolated sites. This stage was associated with peak A in the DSC curve.

21

Because of the extreme reaction velocities exhibited in the SHS reaction in the second stage, the DSC results cannot be used to elucidate the sequential formation of AlNi. However, the initial Al_3Ni phase must follow some sequential conversion to the final AlNi phase. That process is likely much faster than that observed in the DSC measurements and will not follow the observed diffusional growth of the Al_3Ni layer. Moreover, the balance between heat generation and loss is expected to be so different that a precipitation reaction more likely occurs in the SHS process.

In the DSC under slow-controlled anneal conditions, the Al_3Ni nuclei grow in the direction parallel to the Ni/Al interface and subsequently coalescence into a continuous layer. The growth of the Al_3Ni layers in the direction normal to the Ni/Al interface continues until all Al is consumed. However, with increased heat generation in the DSC-heated foils, the mechanism switches from diffusion to a precipitation-controlled process. This stage was related to peak B in the DSC curve. The change in kinetics causes the Al_3Ni to react with the remaining Ni-rich phase to form the final reaction product, AlNi, corresponding to peak C and beyond in the DSC scan.

3.3   Ti-Al Multilayer System

Figure 18 shows the XRD trace of a cold-rolled Ti/Al multilayer foil. In the XRD trace, all the peaks correspond to Ti and Al.
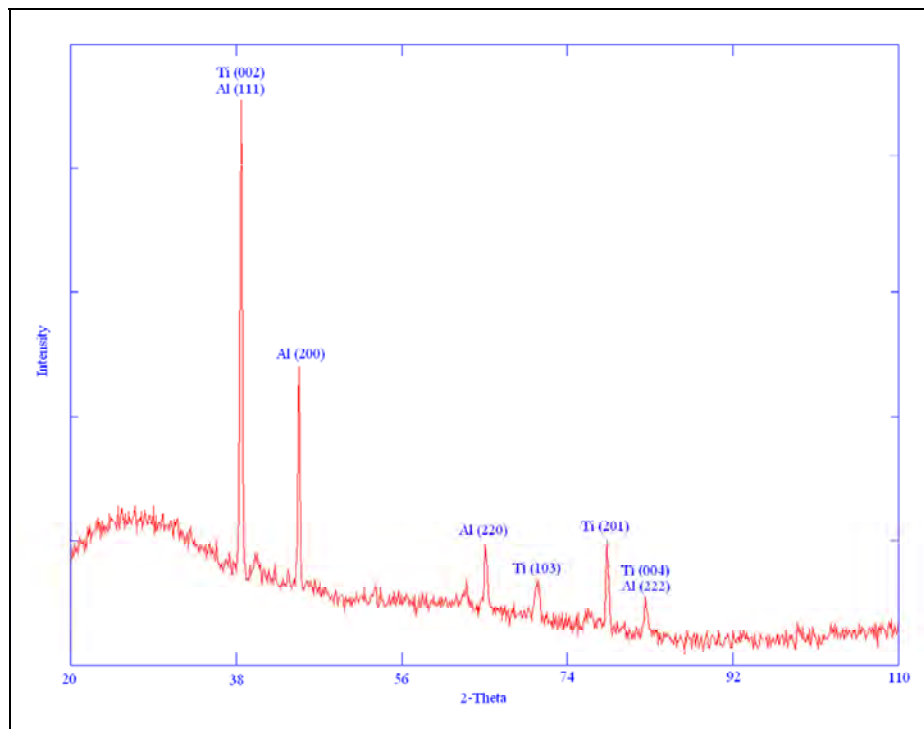

Figure 18. XRD pattern of an as-cold-rolled Ti/Al multilayer foil.

The cold-rolled Ti/Al multilayer foils were ignited with the same method as that used for the Ni/Al multilayer foils. After heating the foil for several seconds, combustion synthesis started in the foil. The reaction in the Ti/Al foils was not self-propagating; this was different from the preceding observations in the Ni/Al foils. Only two reaction stages could be identified. Stage one was a displacement of the reaction zone, where the reaction wave spread along the direction parallel to the surface of the foil, and the foil surface became darker. This stage was similar to that observed in the Ni/Al foils. Then in stage two, the part of the foil immersed in the flame went through thermal explosion. This reaction only occurred in a limited area of the foil that was heated by the flame. The different reaction behaviors of Ni/Al and Ti/Al multilayer foils are due to the different enthalpy of formation of these two systems. The enthalpies of formation for AlNi and AlTi are 59 and 38 kJ/mol, respectively (*19*). Because the reaction between Ti and Al releases much less heat, it cannot sustain a self-propagating reaction in the Ti/Al multilayer foils. Alternative approaches, such as field-activated combustion synthesis (*5*), could be used to achieve SHS in Ti/Al multilayer foils.

Figure 19 shows the cross-sectional SEM images of an as-cold-rolled Ti/Al multilayer foil, the appearance of the foil after the first phase—i.e., the passage of the reaction front of the displacement of the reaction zone—and a foil that experienced thermal explosion. In figure 19a, no sign of reaction can be observed in the as-cold-rolled Ti/Al foil. Polyhedral islands of Ti were embedded in the Al matrix. Unlike the Ni/Al foils, the annealed Ti showed little deformation or necking effect. Instead, it broke into small pieces that were distributed randomly in the Al matrix. After the passage of the front of the displacement of the reaction zone (see figure 19b), a thin layer of Al_3Ti grew epitaxially along the Ti/Al interface, covering the Ti particles entirely. The Ti/Al atomic ratio was obtained by semi-quantitative EDX; it was ~1:3. The appearance of the Ti_3Al layer on the Ti particles is very similar to what happened to the Ni particles in the Ni/Al foils. In agreement with former studies (*34*), Al_3Ti is the first phase to form during the reaction between Ti and Al. As shown in figure 19c, in the final reaction product from the Ti/Al foils, two phases can be identified: a bright Ti-rich phase and a dark Al-rich phase. There are also many globular Al_3Ti particles in the reacted foils, which resulted from the melting of Al during thermal explosion. The Ti/Al compositions at different locations in the reaction product were obtained by EDX and summarized in figure 20. According to the EDX results, different titanium aluminides may be present in the reacted foil. This is due to the nature of thermal explosion. Specifically, during the thermal explosion process, diffusion already occurs during the heating process prior to the onset of the combustion reaction. Consequently, many secondary phases may be present in the final reaction product.

Similar to that for the Ni/Al multilayer foil, we can define the entire reaction process for the cold-rolled Ti/Al multilayer foils by combustion synthesis as follows. First, a displacement of the reaction zone propagated across the foil with formation of Al_3Ti at the Ti/Al interface ($Ti + 3Al \rightarrow Al_3Ti$). Then a thermal explosion reaction occurred in the part of the foil that was put in the flame resulting in many different phases present in the reacted foil.
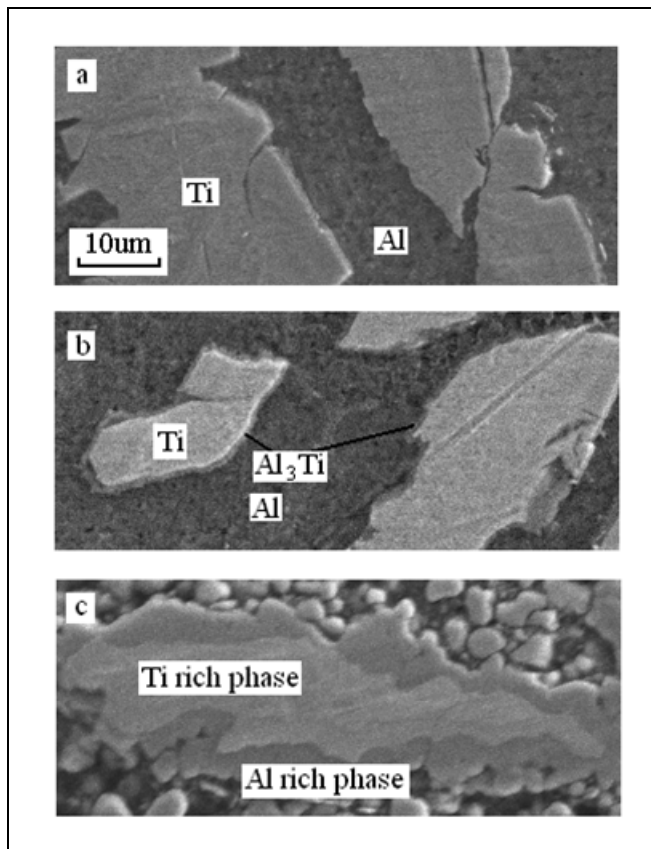
Figure 19. SEM images of the cross-sectional area of cold-rolled Ti/Al multilayer foils: (a) an as-cold-rolled foil, (b) the reaction front of the displacement of reaction zone, and (c) a foil that experienced thermal explosion.
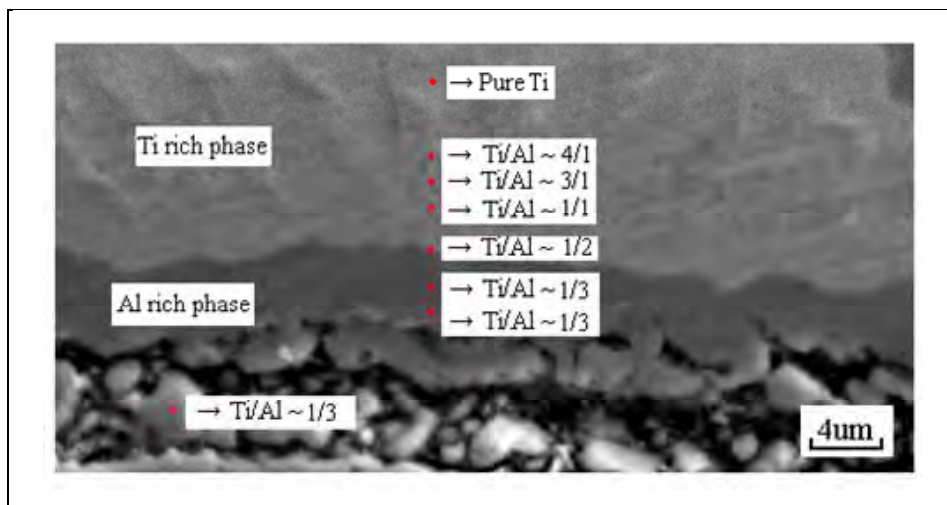

Figure 20. Ti/Al compositions at different locations in the reaction product.

24

4. Conclusions

Ni/Al and Ti/Al multilayer foils were fabricated by a cold-rolling method. In combustion synthesis of cold-rolled foils, Ni/Al foils went through three reaction stages. In the first stage, the reaction spread along the lateral direction to the surface of the foil at a relatively slow rate, and the foil surface became darker. This stage was a displacement of the reaction zone with Al_3Ni as the reaction product. Then the part of the foil in the flame experienced thermal explosion. The subsequent reaction occurred at a much higher speed and released a large amount of heat, emitting visible red light. The heat released triggered an SHS reaction across the foil and resulted in the formation of the final reaction product, AlNi.

Based on a comparison of foils that were partially reacted up to the first stage to those reacted completely, we may conclude that the first SHS reaction stage with a slow reaction velocity is associated with the nucleation and limited lateral growth of the Al_3Ni phase at isolated sites. Further heating under controlled conditions causes these nuclei to coalescence into a continuous layer. Therefore, the second SHS reaction stage with a fast reaction velocity must be the growth of the Al_3Ni layers in the direction normal to the Ni/Al interface until all Al is consumed, with a subsequent reaction of Al_3Ni with the remaining Ni-rich phase to form the final reaction product, AlNi.

DSC experiments showed qualitative agreement with prior models that describe a sequential formation (nucleation and lateral growth) of a single phase in multilayer foils. However, the observed shapes of the exothermic peaks in the DSC profiles from the cold-rolled foils do not agree with the peak shapes used to model the reaction sequence (those obtained from PVD foils). It is likely that the greater separation of the reactants and the nonuniformity of the foil's microstructure have contributed to obscuring the shapes of the exothermic peak doublet. The nonuniform morphology of the cold-rolled foils also alters the nucleation kinetics, wherein a lesser surface area may present itself to available nucleation sites. As such, the initial peak would become broader, thereby reducing the heat that would evolve under the second peak.

For the Ti/Al foils, due to their less enthalpy of formation, only two reaction stages can be identified. First, a displacement of the reaction zone propagated across the foil with formation of Al_3Ti at the Ti/Al interface. Then a thermal explosion reaction occurred in the part of foil that was put in the flame resulting in many different phases present in the reacted foil.

From the fabrication of cold-rolled Ni/Al and Ti/Al multilayer foils, it is clear that the cold-rolling method can be used to fabricate metal/Al multilayer foils and can be potentially extended to fabricate other multilayer systems. With the unique combustion synthesis behaviors, cold-rolled foils provide an ideal opportunity to study the details of the synthesis process in different multilayer systems.

5. References

1. Munir, Z. A.; Anselmi-Tamburini, U. Self-Propagating Exothermic Reactions: The Synthesis of High-Temperature Materials by Combustion. *Mater. Sci. Rep*. **1989**, *3* (7–8), 277–365.

2. Moore, J. J.; Feng, H. J. Combustion Synthesis of Advanced Materials: Part I Reaction Parameters. *Prog. Mater. Sci*. **1995**, *39* (4–5), 243–273, 275–316.

3. Ma, E.; Thompson, C. V.; Clevenger, L. A.; Tu, K. N. Self-Propagating Explosive Reactions in Al/Ni Multilayer Thin-Films. *Appl. Phys. Lett*. **1990**, *57* (12), 1262–1264.

4. Adams, D. P.; Rodriguez, M. A.; Tigges, C. P.; Kotula, P. G.: Self-Propagating, High-Temperature Combustion Synthesis of Rhombohedral AlPt Thin Films. *J. Mater. Res*. **2006**, *21* (12), 3168–3179.

5. Orru, R.; Cao, G.; Munir, Z. A. Mechanistic Investigation of the Field-Activated Combustion Synthesis (FACS) of Titanium Aluminides. *Chem. Eng. Sci*. **1999**, *54* (15–16), 3349–3355.

6. Yi, H. C.; Moore, J. J. Self-Propagating High-Temperature (Combustion) Synthesis (SHS) of Powder-Compacted Materials. *J. Mater. Sci*. **1990**, *25* (2B), 1159–1168.

7. Weihs, T. P. *Handbook of Thin Film Process Technology*; Institute of Physics: Bristol, U.K., 1998.

8. Sieber, H.; Park, J. S.; Weissmüller, J.; Perepezko, H. Structural Evolution and Phase Formation in Cold-Rolled Aluminum-Nickel Multilayers. *Acta. Mater*. **2001**, *49* (7), 1139–1151.

9. Qiu, X.; Wang, J. Experimental Evidence of Two-Stage Formation of Al_3Ni in Reactive Ni/Al Multilayer Foils. *Scripta. Mater*. **2007**, *56* (12), 1055–1058.

10. Battezzati, L.; Pappalepore, P.; Purbiano, F.; Gallino, I. Solid State Reactions in Al Ni Alternate Foils Induced by Cold Rolling and Annealing. *Acta. Mater*. **1999**, *47* (6), 1901–1914.

11. Weihs, T. P.; Reiss, M. Method of Making Reactive Multilayer Foil and Resulting Product. U.S. Patent 6,534,194, 2003.

12. Reiss, M. E.; Esber, C. M.; Van Heerden, D. A.; Gavens, J.; Williams, M. E.; Weihs, T. P. Self-Propagating Formation Reactions in Nb/Si Multilayers. *Mater. Sci. Eng. A*. **1999**, *261* (1–2), 217–222.

13. Wang, J.; Besnoin, E.; Duckham, A.; Spey, S. J.; Reiss, M. E.; Knio, O. M.; Weihs, T. P. Joining of Stainless-Steel Specimens With Nanostructured Al/Ni Foils. *J. Appl. Phys*. **2004**, *95* (1), 248–256.

14. Wang, J.; Besnoin, E.; Knio, O. M.; Weihs, T. P. Effects of Physical Properties of Components on Reactive Nanolayer Joining. *J. Appl. Phys*. **2005**, *97* (11), 114307-1–114307-3.

15. Duckham, A.; Spey, S. J.; Wang, J.; Reiss, M. E.; Weihs, T. P. Reactive Nanostructured Foil Used as a Heat Source for Joining Titanium. *J. Appl. Phys*. **2004**, *96* (4), 2336–2342.

16. Wang, J.; Besnoin, E.; Duckham, A.; Spey, S. J.; Reiss, M.; Knio, O. M.; Powers, M.; Whitener, M.; Weihs, T. P. Room-Temperature Soldering With Nanostructured Foils. *Appl. Phys. Lett*. **2003**, *83* (19), 3987–3989.

17. Swiston, A. J., Jr.; Hufnagel, T. C.; Weihs, T. P. Joining Bulk Metallic Glass Using Reactive Multilayer Foils. *Scripta. Mater*. **2003**, *48* (12), 1575–1580.

18. Wang, J.; Besnoin, E.; Knio, O. M.; Weihs, T. P. Investigating the Effect of Applied Pressure on Reactive Multilayer Foil Joining. *Acta. Mater*. **2004**, *52* (18), 5265–5274.

19. Qiu, X.; Wang, J. Reactive Multilayer Foils for Silicon Wafer Bonding. *Mater. Res. Soc. Symp. Proc*. **2007**, *968* (V02–06).

20. Rabinovich, O. S.; Grinchuk, P. S.; Andreev, M. A.; Khina, B. B. Conditions for Combustion Synthesis in Nanosized Ni/Al Films on a Substrate. *Physica B*. **2007**, *392* (1–2), 272–280.

21. Anselmi-Tamburini, U.; Munir, Z. A. The Propagation of a Solid-State Combustion Wave in Ni-Al Foils. *J. Appl. Phys*. **1989**, *66* (10), 5039–5045.

22. Ma, E.; Thompson, C. V.; Clevenger, L. A. Nucleation and Growth During Reactions in Multilayer Al/Ni Films: The Early Stage of Al_3Ni Formation. *J. Appl. Phys*. **1991**, *69* (4), 2211–2218.

23. Barmak, K.; Michaelsen, C.; Lucadamo, G. Reactive Phase Formation in Sputter-Deposited Ni/Al Multilayer Thin Films. *J. Mater. Res*. **1997**, *12* (1), 133–146.

24. Edelstein, A. S.; Everett, R. K.; Richardson, G. Y.; Qadri, S. B.; Altman, E. I.; Foley, J. C.; Perepezko, J. H. Intermetallic Phase Formation During Annealing of Al/Ni Multilayers. *J. Appl. Phys*. **1994**, *76* (12), 7850–7859.

25. Blobaum, K. J.; Van Heerden, D.; Gavens, A. J.; Weihs, T. P. Al/Ni Formation Reactions: Characterization of the Metastable Al_9Ni2 Phase and Analysis of its Formation. *Acta. Mater*. **2003**, *51* (13), 3871–3884.

26. Sauvage, X.; Dinda, G. P.; Wilde, G. Non-Equilibrium Intermixing and Phase Transformation in Severely Deformed Al/Ni Multilayers. *Scripta. Mater*. **2007**, *56* (1), 181–184.

27. Qiu, X.; Graeter, J.; Kecskes, L.; Wang, J.: Exothermic Reactions in Cold-Rolled Ni/Al Reactive Multilayer Foils. *J. Mater. Res*. **2008**, *23* (2), 367–375.

28. Massalski, T. B., Okamoto, H., Subramanian, P. R., Kacprzak, L., Scott, W. W. Jr., Eds.; *Binary Alloy Phase Diagrams*, 2nd ed.; ASM International: New York, 1992; Vol. 1, pp 181–184, 225–227.

29. Myagkov, V. G.; Zhigalov, V. S.; Bykova, L. E.; Mal'tsev, V. K. Self-Propagating High-Temperature Synthesis and Solid-Phase Reactions in Bilayer Thin Films. *Tech. Phys*. **1998**, *43* (10), 1189–1192.

30. Mann, A. B.; Gavens, A. J.; Reiss, M. E.; Van Heerden, D.; Bao, G.; Weihs, T. P. Modeling and Characterizing the Propagation Velocity of Exothermic Reactions in Multilayer Foils. *J. Appl. Phys*. **1997**, *82* (3), 1178–1188.

31. Gavens, A. J.; Van Heerden, D.; Mann, A. B.; Reiss, M. E.; Weihs, T. P. Effect of Intermixing on Self-Propagating Exothermic Reactions in Al/Ni Nanolaminate Foils. *J. Appl. Phys*. **2000**, *87* (3), 1255–1263.

32. Coffey, K. R.; Clevenger, L. A.; Barmak, K.; Rudman, D. A.; Thompson, C. V. Experimental Evidence for Nucleation During Thin-Film Reactions. *Appl. Phys. Lett*. **1989**, *55* (9), 852–854.

33. Pretorius, R.; Vredenberg, A. M.; Saris, F. W.; de Reus, R. J. Prediction of Phase Formation Sequence and Phase-Stability in Binary Metal-Aluminum Thin-Film Systems Using the Effective Heat of Formation Rule. *Appl. Phys*. **1991**, *70* (7), 3636–3646.

34. Van Loo, F. J. J.; Rieck, G. D. Diffusion in Titanium-Aluminum System. 1. Interdiffusion Between Solid Al and Ti or Ti-Al Alloys. *Acta. Mater*. **1973**, *21* (1), 61–71.

NO. OF
COPIES   ORGANIZATION

1   DEFENSE TECHNICAL
(PDF   INFORMATION CTR
only)   DTIC OCA
        8725 JOHN J KINGMAN RD
        STE 0944
        FORT BELVOIR VA 22060-6218

1   DIRECTOR
        US ARMY RESEARCH LAB
        IMNE ALC HRR
        2800 POWDER MILL RD
        ADELPHI MD 20783-1197

1   DIRECTOR
        US ARMY RESEARCH LAB
        RDRL CIM L
        2800 POWDER MILL RD
        ADELPHI MD 20783-1197

1   DIRECTOR
        US ARMY RESEARCH LAB
        RDRL CIM P
        2800 POWDER MILL RD
        ADELPHI MD 20783-1197

1   DIRECTOR
        US ARMY RESEARCH LAB
        RDRL D
        2800 POWDER MILL RD
        ADELPHI MD 20783-1197

        ABERDEEN PROVING GROUND

1   DIR USARL
        RDRL CIM G (BLDG 4600)

INTENTIONALLY LEFT BLANK.